Dispersion-Enhanced Photonic Crystal Fiber Array for a True Time-Delay Structured X-Band Phased Array Antenna

Yongqiang Jiang, *Student Member, IEEE*, Brie Howley, Zhong Shi, Qingjun Zhou, Ray T. Chen, *Fellow, IEEE*, Maggie Y. Chen, George Brost, and Charles Lee

***Abstract*—Tunable optical true time-delay modules based on highly dispersive photonic crystal fibers (PCFs) are demonstrated to provide continuous radio-frequency squint-free beam scanning for an X-band (8–12 GHz) phased array antenna system. The dispersion of the fabricated PCF is as high as -600 ps/nm · km at 1550 nm. The time delay is continuously tunable from -31 to 31 ps between adjacent delay lines by tuning the laser wavelength continuously from 1528 to 1560 nm. The far field radiation patterns of a 1×4 subarray were measured from $-45°$ to $45°$ scanning angles. Squint-free operation is experimentally confirmed.**

***Index Terms*—Optical true time delay (TTD), phased array antenna (PAA), photonic crystal fiber (PCF), wavelength tuning.**

I. Introduction

PHASED ARRAY antennas (PAAs) have the advantages of high directivity and quick beam steering without physical movement. Each antenna element of a PAA must have the correct phase condition to accomplish the desired beam scanning. However, the conventional electrical phase trimmer technique is intrinsically narrow-band and introduces beam squint. Recently, there has been growing interest in optical true time-delay (TTD) techniques with the features of wide bandwidth, compact size, reduced system weight, and low electromagnetic interference when compared with electrical TTD techniques [1], [2]. However, most of the optical TTD techniques require a large number of precisely time-delay-matched optical elements such as lasers and optical delay segments resulting in a complex system design. Esman *et al.* proposed a fiber-optic TTD technique using conventional dispersion compensating fiber (DCF) to meet these requirements [2]. However, its dispersion parameter D of conventional DCF is of fairly small magnitude ($D = -100$ ps/nm · km), and therefore, long lengths of it are still needed in the TTD module to get the required delay. If the fiber group velocity dispersion is increased, the total fiber length will be decreased proportionally.

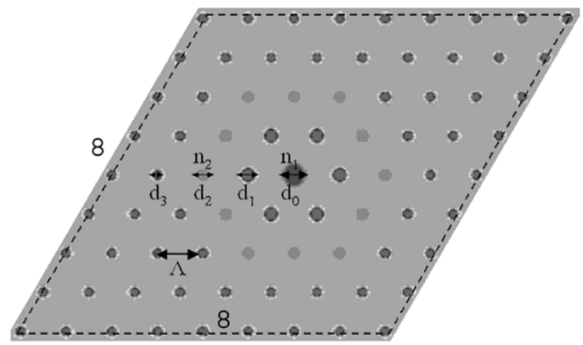

Fig. 1. Transverse section of a model highly dispersive PCF. The box with dimensions $D \times D$ corresponds to the supercell used to implement boundary conditions.

Conventional single-mode fibers (SMFs), based on weakly guiding structures of doped silica, can be tailored slightly to increase the dispersion by increasing the refractive index difference between the core and cladding [3]. However, dispersion cannot be changed significantly because of the small index variation across the transverse cross section from doping. This shortcoming can be overcome by the employment of high dispersion photonic crystal fibers (PCFs). PCFs have generated a lot of interest due to their unusual and attractive properties [3]–[7]. They are usually made of silica or polymer material with a regular hexagonal array of submicrometer-sized air holes running along the fiber as a cladding. A defect, usually one or multiple missing holes, acts as core. The dispersion of the PCFs is tuned by changing the pitch (Λ) of the periodic array, the hole diameter (d) and the doping concentration (n) of the core, as shown in Fig. 1, [3]–[5].

In this letter, we implement a novel optical TTD module using an array of highly dispersive PCF. The TTD module is designed, fabricated, and evaluated. The approach is based on highly dispersive PCF reported herein and other commercially available components and has potentially high reliability and stability as it requires no physically moving parts and no critical optical alignments. This is the first system demonstration to employ PCF-based TTD modules for control of an X-band PAA system. The radio-frequency (RF) phase as the function of RF frequency is measured to verify that the time delay is independent of RF frequency. The wide instantaneous bandwidth of the TTD

Manuscript received June 23, 2004; revised August 7, 2004. The X band testbed of the antenna system was supported by the Air Force Office of Scientific Research (AFOSR) and by the Missile Defense Agency (MDA). The X band phased array antenna array was provided by the Air Force Research Laboratory (AFRL). The photonic crystal fiber work reported herein for the true time delay application is currently supported by the Defense Advanced Research Project Agency (DARPA).

Y. Jiang, B. Howley, Z. Shi, Q. Zhou, and R. T. Chen are with the Microelectronic Research Center, Department of Electrical and Computer Engineering, The University of Texas at Austin, Austin, TX 78758 USA (e-mail: chen@ece.utexas.edu).

M. Y. Chen is with Omega Optics, Austin, TX 78758 USA.

G. Brost is with the Air Force Research Laboratory, Rome, NY 13440 USA.

C. Lee is with the Air Force Office of Scientific Research (AFOSR), Arlington, VA 22203 USA.

Digital Object Identifier 10.1109/LPT.2004.838623

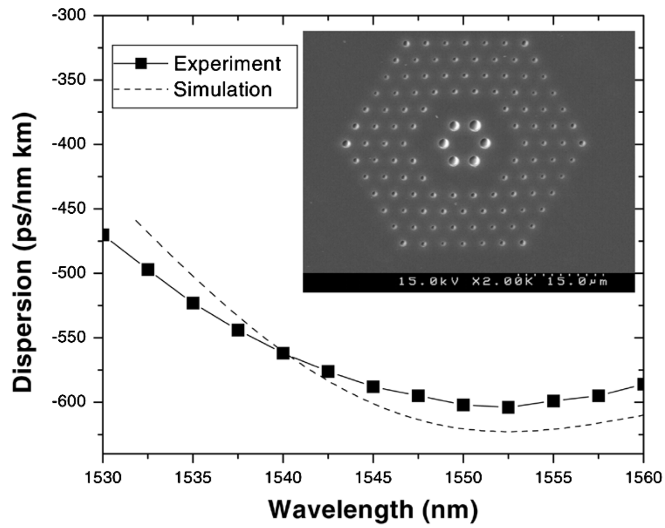

Fig. 2. Simulated and measured chromatic dispersion parameter D for highly dispersive PCFs. Insert is an SEM image of the fabricated highly dispersive PCF.

module is confirmed by measurements of the far-field patterns of the X-band PAA at two X-band frequencies.

II. TTD Module Design, Fabrication, and Characterization

We use a two-core PCF design to achieve high dispersion. The inner core is a doped silica rod instead of a missing hole, and the outer core is 12 concentric doped silica rods instead of missing holes, as shown in Fig. 1. Both cores are doped to have higher refractive index than pure silica, but the refractive index of the inner core is greater than that of the outer core. This two-core PCF can support two supermodes, which are analogous to the two supermodes of a directional coupler [6]. These modes are nearly phase matched at 1550 nm. Close to the phase matching wavelength, the mode index of the PCF changes rapidly due to strong coupling between the two individual modes of the inner core and outer core. Due to strong refractive index asymmetry between the two cores, there is a rapid change in the slope of the wavelength variation of the fundamental mode index. This leads to a large dispersion around 1550 nm. The air-hole structure helps not only to guide the mode, but also to increase the dispersion value [6].

The dispersion of PCFs can be calculated using the full vectorial plane-wave expansion (PWE) method, which is fast and accurate compared to other methods [7]. Since our PCF design is not a perfect crystal without defects, we need to use a supercell having a size of $N \times N$ instead of a natural unit cell to implement the periodic boundary conditions [7]. As shown in Fig. 1, an 8×8 supercell is used for simulation purposes. Here, 8×8 meets the simulation convergence compared with 7×7 and 9×9.

The dispersion parameter $D(\lambda)$ of PCF is strongly related to the structure and refractive index perturbation, and can, thus, be changed to achieve the desired characteristics [3]–[5]. In our design, we use different doping concentrations, $\Lambda, d_0, d_1, d_2, d_3$, as shown in Fig. 1, to tune the dispersion.

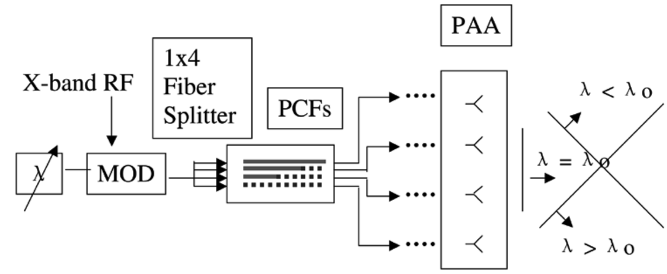

Fig. 3. Highly dispersive PCF enhanced wavelength continuous tunable PAA system structure. (Dashed line: Highly dispersive PCF. Solid line: Lucent TrueWave SMF. MOD: Modulator).

Here, d_0 and d_2 are the diameters of the inner and outer doped silica rods, respectively, and d_1 and d_3 are the diameters of the air holes. Fig. 2 shows the theoretical simulation results of highly dispersive PCFs using the PWE method. The highest dispersion about -630 ps/nm $\cdot$ km is obtained at 1552.5 nm. The highly dispersive PCF is fabricated using the stack-and-draw technique, where silica glass capillaries are stacked in a desired lattice array, fused together, and then drawn down to PCF. [4]. The scanning electron micrograph (SEM) image of the cross section is shown in the insert of Fig. 2. In order to measure the chromatic dispersion of the fabricated highly dispersive PCFs, we measured the time delay between optical wavelengths of $\lambda_o \pm 0.1$ nm. To obtain the time delay, we measured the phase difference between optical wavelengths ($\lambda_o + 0.1$ nm) and ($\lambda_o - 0.1$ nm) that are modulated at different microwave frequencies. The time delay can be derived from the slope of each curve. The fiber chromatic dispersion is defined as $\Delta T/(\Delta\lambda \cdot L)$, which can be obtained from the time delay divided by fiber length and laser wavelength difference 0.2 nm. The dispersion is -600 ps/nm $\cdot$ km at 1550 nm, as shown in Fig. 2. The dispersion is increased by 33 times compared to telecom SMF-28 which has a dispersion parameter of 18 ps/nm $\cdot$ km, and by six times compared to conventional DCF. Since the material of the PCF is silica glass, the environmental stability of the dispersion of the PCF is similar to conventional silica fiber.

A 1×4 TTD module is designed and assembled using the fabricated highly dispersive PCF delay lines mentioned above. The lengths of the highly dispersive PCFs are 10.5, 7.0, 3.5, and 0 m, as shown in Fig. 3. The measured insertion losses of the delay lines are 3.4, 3.3, 3.2, 0.5 dB, respectively. Each delay line has the same nominal group delay at the central tuning wavelength 1545 nm but with slightly different net dispersion. This can easily be constructed by connecting varying lengths of highly dispersive PCFs and Lucent TrueWave SMF ($D \approx$ 3 ps/nm $\cdot$ km from 1530 to 1565 nm). The relative delay of the signals among the delay lines can, thus, be changed by tuning the optical wavelength. At the central tuning wavelength λ_0 1545 nm, all the time delays are matched by trimming the TrueWave SMF. Thus, at λ_0, the main antenna beam will be directed broadside. At wavelengths deviating from λ_0, each of the fiber delay lines generates a time delay proportional to its dispersion parameter D and the highly dispersive PCF length, resulting in a phase change to steer the main antenna radiation beam [2].

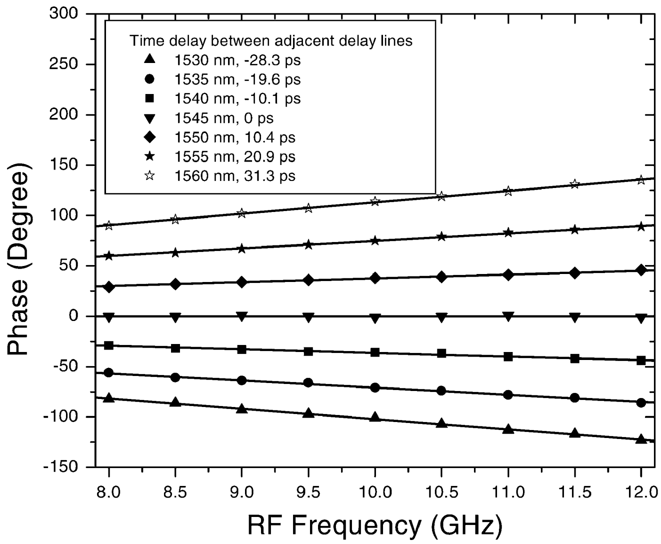

Fig. 4. Measured phase as a function of frequency. The time delays between two adjacent delay lines are calculated from the slope of the phase versus RF frequency.

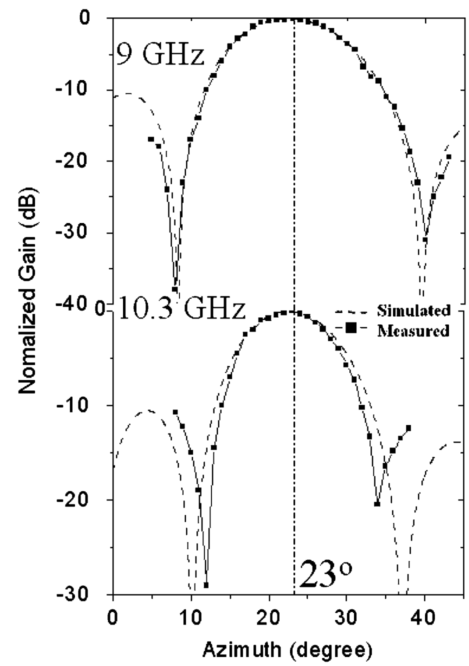

Fig. 5. Comparison of far-field patterns of the PAA at 23° scanning angle at frequencies of 9 and 10.3 GHz with an optical wavelength of 1553 nm.

The measured phase difference versus modulation frequency curves at different wavelengths are shown in Fig. 4. The time delay shown in the inset is derived from the slope of each curve. The wavelength at 1545 nm was chosen as a reference for zero time delay. By tuning the wavelength from 1528 to 1560 nm, different time delays can be achieved ranging from −31 to 31 ps between any two adjacent delay lines. This is equivalent to scanning angles ranging from −45° to 45° for a two-bit four-element PAA subarray having half-wavelength spacing at 10 GHz. The linearity of phase versus frequency curve verifies the true-time delay and wide bandwidth capability of the proposed scheme.

III. System Measurement

The assembled four-element X-band PAA system is demonstrated and the block diagram is shown in Fig. 3. A microwave signal is generated from the HP network analyzer [8]. The optical carrier from the tunable laser (tuning range: 1520–1580 nm; spectral width: 200 MHz; tuning resolution: $<$0.024 nm) is distributed into the four subunits of the TTD delay lines by a one-to-four fiber splitter. After the predetermined time delay, the optical signals with correct phase relationships are detected by InGaAs high-speed photodetectors and individually fed into four antenna elements after amplification.

The far-field pattern of the PAA is measured to verify the instantaneous RF broad-band characteristics at frequencies of 9 and 10.3 GHz. Fig. 5 shows the far-field patterns at 23° scanning angle corresponding to a 17-ps delay time using a laser wavelength of 1553 nm (compared to the reference wavelength of 1545 nm that results in 0° scanning). From Fig. 5, it can be seen that the simulation results and measured data agree fairly well. The deviation from the theoretical prediction shown in Fig. 5 is due to the nonuniformity of the four radiation elements. As expected, the measurement shows no beam squint effect.

IV. Conclusion

A novel true-time delay module using highly dispersive PCFs has been designed, fabricated, and experimentally evaluated in an X-band phased-array antenna system. This module is compact, low loss, and easy to package while providing wide instantaneous bandwidth. The ultimate application of this approach is limited by the tuning speed of the tunable laser. Wipiejewski *et al.* report a tunable laser with 40-ns tuning speed, which is fast enough for most PAA applications [9]. Due to the maturity of the tunable laser in 1550-nm region, the wavelength tuning is feature free for the tuning range of 60 nm at least. By increasing the dispersion of the PCF, the required tuning bandwidth of the tunable laser can also be decreased.

References

[1] W. Ng *et al.*, "The first demonstration of an optically steered microwave phased array antenna using true-time-delay," *J. Lightw. Technol.*, vol. 9, no. 9, pp. 1124–1131, Sep. 1991.

[2] R. D. Esman *et al.*, "Fiber-optic prism true time-delay antenna feed," *IEEE Photon. Technol. Lett.*, vol. 5, no. 11, pp. 1347–1349, Nov. 1993.

[3] L. P. Shen *et al.*, "Design and optimization of photonic crystal fibers for broad-band dispersion compensation," *IEEE Photon. Technol. Lett.*, vol. 15, no. 4, pp. 540–542, Apr. 2003.

[4] J. A. West *et al.*, "Photonic crystal fibers," in *Proc. 27th Eur. Conf. Opt. Commun. (ECOC 2001)*, vol. 4, 2001, pp. 582–585.

[5] Y. Jiang *et al.*, "Highly dispersive photonic crystal fibers for true-time-delay modules of an X-band phased array antenna," *Proc. SPIE*, vol. 5360, pp. 40–59, 2004.

[6] K. Thyagarajan, R. K. Varshney, and P. Palai, "A novel design of a dispersion compensating fiber," *IEEE Photon. Technol. Lett.*, vol. 8, no. 11, pp. 1510–1512, Nov. 1996.

[7] J. Broeng *et al.*, "Analysis of air-guiding photonic bandgap fibers," *Opt. Lett.*, vol. 25, pp. 96–98, 2000.

[8] Z. Shi, Y. Jiang, B. Howley, Y. Chen, F. Zhao, and R. T. Chen, "Continuously delay-time tunable-waveguide hologram module for X-band phased-array antenna," *IEEE Photon. Technol. Lett.*, vol. 15, no. 7, pp. 972–974, Jul. 2003.

[9] Y. Wipiejewski, Y. A. Akulova, and C. Schow, "Monolithic integration of a widely tunable laser diode with a high speed electro absorption modulator," in *Proc. Electronic Components Technology Conf.*, 2002, pp. 558–562.